Fast growth of GaN epilayers via laser-assisted metal-organic chemical vapor deposition for ultraviolet photodetector applications

Hossein Rabiee Golgir, Dawei Li, Kamran Keramatnejad, Qi Ming Zou, Jun Xiao, Fei Wang, Lan Jiang, Jean-François Silvain, Yong Feng Lu

Fast Growth of GaN Epilayers via Laser-Assisted Metal Organic Chemical Vapor Deposition for Ultraviolet Photodetector Applications

Hossein Rabiee Golgir,[†,±] Da Wei Li,[†,±] Kamran Keramatnejad,[†] Qi Ming Zou,[†] Jun Xiao,[†] Fei Wang,[£] Lan Jiang,[‡] Jean-François Silvain,[§] and Yong Feng Lu[†,]*

[†]Department of Electrical and Computer Engineering, University of Nebraska-Lincoln, Lincoln, NE 68588-0511, USA

[£]Department of Mechanical & Materials Engineering, University of Nebraska–Lincoln, Lincoln, NE 68588-0511, USA

[‡]School of Mechanical Engineering, Beijing Institute of Technology, Beijing 100081, China

[§]Institut de Chimie de la Matière Condensée de Bordeaux (ICMCB-CNRS) 87, Avenue du Docteur Albert Schweitzer F-33608 Pessac Cedex, France

ABSTRACT: In this study, we successfully developed a carbon dioxide (CO_2) laser-assisted metal organic chemical vapor deposition (LMOCVD) approach to fast synthesis of high-quality gallium nitride (GaN) epilayers on Al_2O_3 (sapphire (0001)) substrates. By employing a two-step growth procedure, high crystallinity and smooth GaN epilayers with a fast growth rate of 25.8 μm/h were obtained. The high crystallinity was confirmed by a combination of techniques including X-ray diffraction, Raman spectroscopy, transmission electron microscopy and atomic force microscopy. By optimizing growth parameters, the ~ 4.3 μm thick GaN films grown at

990 °C for 10 min showed a smooth surface with a root mean square surface roughness of ~ 1.9 nm and excellent thickness uniformity with sharp GaN/substrate interfaces. The full-width at half-maximums of GaN (0002) X-ray rocking curve of 313 arcsec and GaN (10-12) X-ray rocking curve of 390 arcsec further confirmed the high crystallinity of GaN epilayers. We also fabricated ultraviolet (UV) photodetectors based on the as-grown GaN layers, which exhibited a high responsivity of 0.108 AW^{-1} at 367 nm and a fast response time of ~ 125 ns, demonstrating its high optical quality with potential in optoelectronic applications. Our strategy thus provides a simple and cost-effective means toward fast and high-quality GaN hetero-epitaxy growth suitable for fabricating high-performance GaN-based ultraviolet (UV) detectors.

KEYWORDS: LMOCVD, GaN epilayer, fast growth, ultraviolet photodetector

Gallium nitride (GaN) with excellent physical properties, such as wide direct bandgap, high electron mobility and high thermal stability, has been extensively studied and attracted attentions for applications in light-emitting diodes (LEDs), high-power electronic devices and short wavelength optoelectronics.[1-3] Current commercial GaN-based devices are fabricated by epitaxy onto foreign substrates because the GaN bulk and freestanding substrate technology is still immature.[4] High-quality GaN are routinely grown by hydride vapor phase epitaxy (HVPE), ammonothermal, molecular beam epitaxy (MBE), and metal-organic chemical vapor deposition (MOCVD).[5-11] Although HVPE and ammonothermal methods with the advantage of high growth rates have emerged to obtain bulk GaN,[5-7] they lack the precise control and heterojunction layer growth required for device structures. The overwhelming majority of GaN epilayers and GaN-based devices are grown by MOCVD and MBE.[8-12] The MOCVD growth rate of GaN epilayers commonly exceeds 1–3 μm/h, while MBE is typically performed with a growth rate up to 1 μm/h.[8-12] The relatively slow growth rates limit these traditional methods for many device structures that require thick GaN layers. Therefore, synthetic techniques with high growth rates are highly in demand for the scalable production of high-quality GaN epilayers to satisfy the steadily increasing requirement, since it can help reducing the cycle time in device fabrication.

Laser-assisted MOCVD (LMOCVD) is an ideal method for various material growth with advantages of low growth temperature, fast growth rate, and the capability to deposit patterned materials.[13-20] Several semiconductor materials, including silicon, gallium arsenide, indium phosphide, and aluminum nitride, have been successfully grown using LMOCVD.[13-17] For instance,

Zhou *et al*.[21] reported ultraviolet laser LMOCVD growth of c-oriented GaN films with a broad XRD peak at low temperatures. However, the photolysis of the precursors with UV laser resulted in the low density of the reactive radicals and a slow GaN growth rate. On the other hand, CO_2 laser LMOCVD has been successfully used to prepare various kinds of thin films at high growth rates.[16, 22-30] For instance, Iwanaga *et al*.[22] reported the deposition of large-area amorphous silicon films using CO_2 laser LMOCVD with a high growth rate of > 60 μm/h in a relatively low laser power and low substrate temperatures. Recently, we have demonstrated the fast growth of GaN films with (0002) preferential orientation using CO_2 laser LMOCVD with a growth rate up to 84 μm/h at low temperatures,[26] where the experiments were designed to elucidate the GaN growth mechanism via CO_2 laser LMOCVD rather than to optimize the material crystalline quality. The high GaN growth rate is due to the mixed photolysis/pyrolysis reactions of the precursors and the photo-induced effects, as has been evidenced by wavelength dependence of GaN growth rates.[25-27] However, the low-temperature deposition resulted in films with broad XRD peaks and low crystalline quality.[22, 25] The growth of high-quality GaN films suitable for device application were usually realized at high deposition temperatures.[31-34]

In this study, we successfully demonstrated the fast growth of high-quality GaN epilayers on sapphire substrates with a growth rate of 25.8 μm/h using an optimized CO_2 laser LMOCVD method. The growth of GaN epilayers followed previously documented two-step growth steps,[35] including a thin three dimensional (3D) GaN layer growth, lateral growth and coalescence of the 3D layer, and finally quasi-two dimensional (2D) growth at high temperatures. The growth rate of

25.8 μm/h is 8.6 times higher than that has been used in GaN epliayers by traditional MOCVD.[11-12] This work presents an efficient and low-cost means to realize fast and high-quality GaN epilayer growth with potential applications in GaN-based optoelectronics.

METHODS

Growth of GaN epilayers: The growth of GaN epilayers on (0001) orientation sapphire substrates was performed in a home-made vertical LMOCVD system (Figure 1a). Trimethylgallium (TMGa) and ammonia (NH_3) were used as gallium and nitrogen precursors, respectively. The 1×1 cm^2 sapphire substrates were successively cleaned in piranha and 15% hydrochloric acid solution before loading into the LMOCVD system for the GaN growth. A continuous-wave (CW) and wavelength-tunable CO_2 laser (PRC Inc., $\lambda = 9.201$ μm) was used for substrate heating. A flat-top laser beam shaper (Edmund Optics) was used to generate a beam with uniform power distribution (output beam diameter ~ 20 mm) from a Gaussian CO_2 laser beam (Figure 1a), in order to realize a uniform substrate temperature for material growth with controlled crystal orientations. The chamber pressure during the growth was kept at ~ 10 Torr. A two-step growth procedure was used for the synthesis of high-quality and smooth GaN epilayers without using AlN buffer layers.[35] NH_3 (26 mmol/min) and TMGa (20 μmol/min) were introduced into the chamber after the substrate temperature was stable under laser irradiation. The growth process started with deposition of a very thin 3D GaN layer (~ 7-10 nm) for 10 s at 700 ºC with a laser power of ~ 95 W. After that the growth was stopped and the 3D GaN layer was annealed at 990 ºC for 5 min (laser power ~ 160 W) under NH_3 with a flow rate of 26 mmol/min. The subsequent growth of unintentionally doped

GaN epilayer was carried out at temperatures ranging from 930 to 990 °C by adjusting laser power for 10 min. The substrate temperature during the growth was monitored by a pyrometer (Omega, OS3752).

Characterization: The morphology of the GaN layers was investigated using atomic force microscopy (AFM, Bruker Dimension ICON SPM) and scanning electron microscopy (SEM, S4700). The structural properties of the GaN epilayers were examined using high-resolution X-Ray diffraction (HR-XRD, Rigaku SmartLab), Raman spectroscopy and transmission electron microscopy (TEM, FEI Tecnai OsirisTM, 200 kV). The samples for cross-sectional TEM characterization were prepared as follows. Firstly, the GaN sample was coated with a 20-nm-thick Ti film to prevent ion-beam damage to the sample surfaces during the FIB processing. Secondly, Ga+ ion beams with energies of 30 and 10 keV were used for bulk milling and polishing of Ti-coated GaN sample, respectively, in an FEI Helios NanoLab 660 FIB/SEM system. Finally, the GaN lamellae with a thickness of ~ 60-100 nm was mounted on the TEM grids. HR-XRD characterization was performed using Rigaku Smart Lab Diffractometer with Cu Ka1 radiation (l = 1.5406 Å). Raman spectra were collected in a micro-Raman system (Renishaw inVia) using a 514.5 nm Ar^+ laser as irradiation source. Hall effect measurements were performed using Van der Pauw method. Optical transmission spectra were measured via a UV/Vis/NIR spectrometer (Perkin-Elmer LAMBDA 1050).

Fabrication and characterization of GaN metal-semiconductor-metal (MSM) UV photodetectors: GaN devices were fabricated using a standard photolithography: 1) patterning of

photoresist, 2) deposition of Ni/Au (100 nm/20 nm) Schottky contact via magnetron sputtering, and 3) lift-off to form Schottky contacts (50 μm long, 10 μm wide with a spacing of 10 μm) on GaN. Before electrical measurement, annealing treatment of GaN MSM devices was performed at 500 °C for 5 min in rapid thermal processing (RTP) furnace. The current-voltage (*I-V*) measurements of the GaN UV photodetectors were carried out using a Keithley 237 electrometer. Photoresponse measurements were realized by using a Xe arc lamp with power of 150 W as UV light source. External quantum efficiency (EQE) measurement was performed by using an incident monochromatic light beam directed onto the photodetector and the data was collected via a Newport QE measurement kit. Transient response measurements were taken using a 337 nm, 4 ns pulsed laser as light source, and voltage variations were collected using an oscilloscope (LeCroy WaveRunner).[36-38] All measurements were conducted at room temperature.

RESULTS AND DISCUSSION

Figure 1a shows the schematic LMOCVD system used for fast and high-quality GaN epilayer growth on sapphire substrates. The cross-sectional SEM image in Figure 1b is a typical LMOCVD GaN sample grown at 990 °C for 10 min on sapphire, which shows a very sharp hetero-interface between GaN layer and substrate. The thickness of the GaN epilayer was measured to be ~ 4.3 μm, corresponding to a growth rate of ~ 25.8 μm/h which is much higher than that of the conventional techniques for GaN epilayer growth (~ 1 μm/h for MBE and ~ 3 μm/h for MOCVD), as shown in Figure 1c. [8-12] Moreover, the total growth process for LMOCVD was less than 20 min, as compared with several hours needed for the HVPE, ammonothermal, MOCVD, and MBE

methods.[5-12] The thicknesses of GaN layers grown at 930 and 960 °C for 10 min were calculated to be ~ 3.85 and 4.12 µm, respectively, revealing an increase in growth rates as a function of deposition temperature.

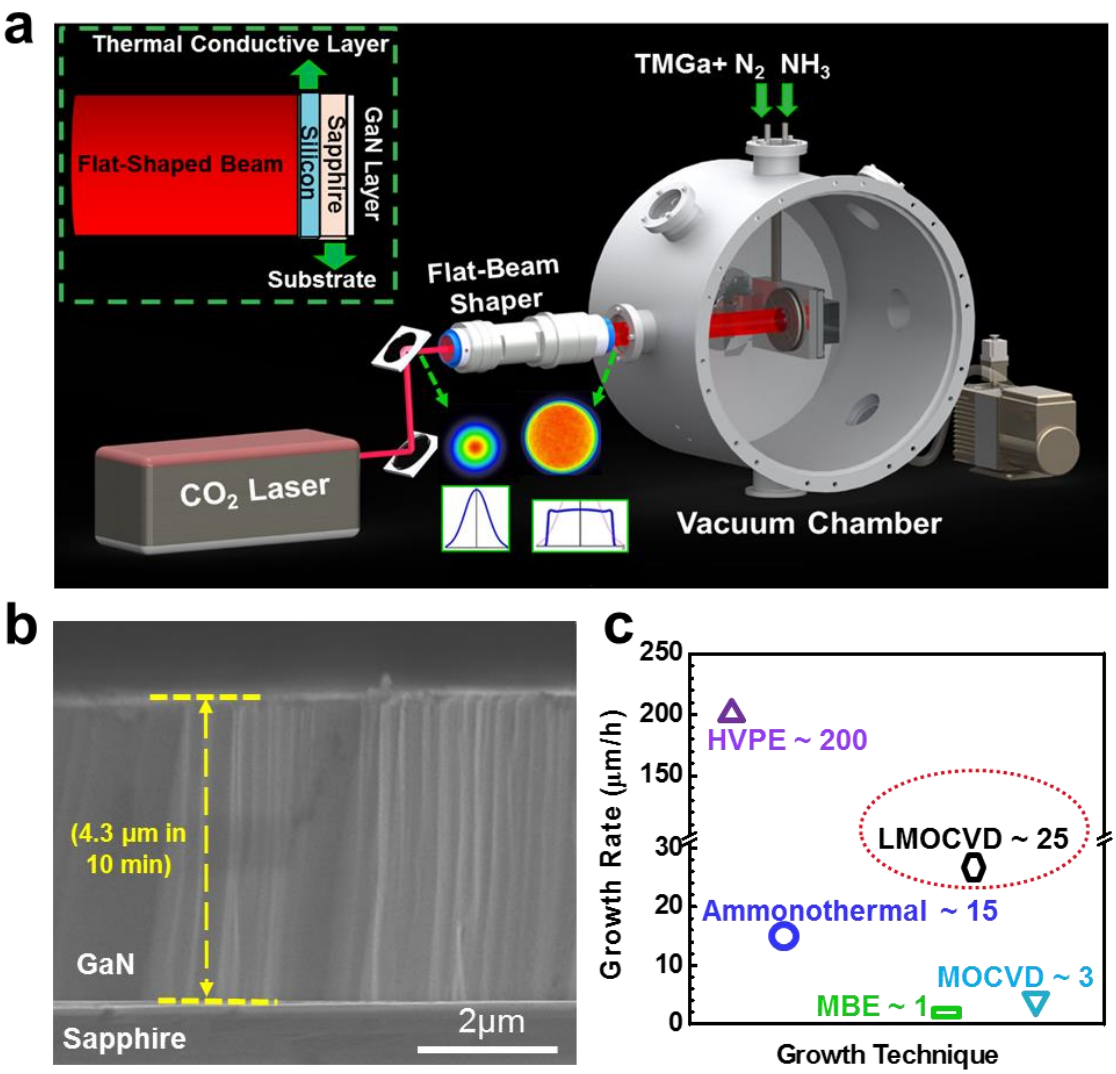

Figure 1. (a) Schematic of the experimental setup of CO_2 laser LMOCVD system. (b) Cross-sectional SEM image of the ~ 4.3 µm thick GaN epilayer grown on a sapphire (0001) substrate at 990 °C for 10 min. (c) A comparison of growth rate between different techniques used for growth of high-quality GaN.

Morphological evolution of GaN during the growth process was investigated, as shown in Figure 2. In step 1, very thin GaN 3D islands with a thickness of ~ 7-10 nm were grown at 700 °C. After

annealing at 990 ^{o}C for 5 min under the NH_3 flow, the GaN islands grew up laterally, and started to coalesce gradually. In step 2, with the increasing in the growth time at high temperature (HT) growth, the GaN islands increased in sizes and grew into a continuous and smooth film followed by a rapid coalescence.[39] Figures 2a and 2b show the top views of GaN islands after 30 and 90 s HT growth, respectively. It is notable that the sizes and morphologies of the GaN islands are relatively uniform after 90 s HT growth. The coalescence of GaN islands was completed after ~ 120 s HT growth by forming pits with inverted hexagonal pyramid shape (IHP). The IHP defects subsequently disappeared during further HT growth step (not shown here). Figures 2c shows the SEM image of the GaN epilayers after 10 min HT growth. It is clear that the 3D island coalescence switched to a 2D step growth mode over the whole substrate. The AFM image of a fully coalesced GaN epilayer in Figure 2d shows a smooth morphology with spiral hillocks, which is similar to that of high-quality GaN grown by the MOCVD and MBE methods with much lower growth rates.[9, 40] AFM measurement further revealed that the surface root-mean-square (RMS) roughness for the GaN epilayers grown at 990 ^{o}C is as small as 1.892 nm, slightly higher than that of the reported works with much lower growth rates.[9, 40-41] The GaN with smooth surface is of great importance for the design and fabrication of high-performance GaN-based optical and optoelectronic devices. The RMS roughness for GaN layers grown at 930 and 960 °C was measured to be 1.103 and 1.253 nm (Figure S1), respectively, revealing a smoother GaN growth at relatively lower temperatures in this work.

The cross-sectional TEM image of the GaN epilayers grown at 990 °C is shown in Figure 2e. It was observed that the as-grown GaN has a single-crystalline structure with an epitaxial layer even at the interface of GaN and sapphire substrate. The lattice fringes has a spacing of ~ 0.517 nm, which is consistent with the GaN *c*-plane interplanar distance.[42] The (0002) lattice fringes are parallel to the substrate surface. Figure 2f shows a selected-area electron diffraction (SAED) pattern of the GaN epilayer, which revealed the single crystal array of spots indexed to the reflection of GaN with the wurtzite structure along the (0001) direction. Furthermore, the regularity of the atomic arrangement and the absence of a diffuse streak demonstrated the highly crystalline nature of the GaN epilayers.[42]

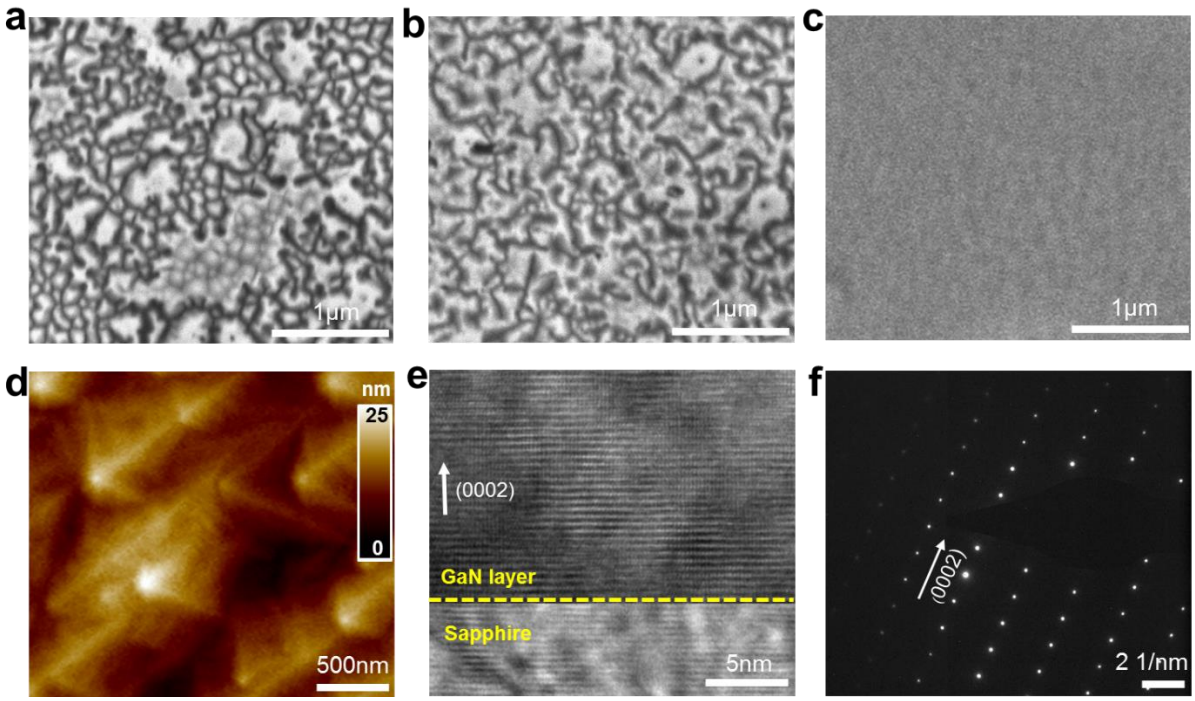

Figure 2. Morphological and structural characterization of GaN epilayers grown on sapphire substrates. (a-c) SEM plan views of GaN during growth process: (a) GaN islands after 30 s HT growth, (b) GaN islands after 90 s HT growth, and (c) GaN epilayers after 10 min HT growth. (d) AFM image for GaN epilayer grown at HT for 10 min with an average surface roughness of ~ 1.9 nm. (e) High-resolution cross-sectional TEM image for the GaN/sapphire hetero-interface. (f) Selected-area diffraction pattern for the GaN epilayer.

XRD was performed to study the structural properties of the GaN epilayers grown on sapphire. Figure 3a compares XRD 2θ scans for the GaN epilayers grown on sapphire at different temperatures. Two peaks at around 34.51 and 72.64 were identified in each spectrum, which are indexed to the reflections of wurtzite GaN (0002) and (0004), respectively. Therefore, the out-of-plane epitaxial relationship of GaN (0001) and sapphire substrate were determined for these samples. Furthermore, it can be observed that the GaN (0002) and (0004) peak intensities are gradually increased and the peaks become sharper as the GaN growth temperature increases from 930 to 990 °C, revealing the improved crystalline quality of the GaN epilayers at higher temperature. XRD φ scan was conducted to examine the in-plane epitaxial relationship between GaN epilayers and sapphire substrates, while 2θ was constant for the peak position and the GaN sample was rotated 360º around the surface normal. The scanning planes used for φ scan were hexagonal (10-12) and (11-20) for GaN layers and sapphire, respectively. Figure 3b shows the normalized φ scans of GaN (10-12), where the diffraction peaks with an interval of 60° are observed for all the samples. The variation in the peak intensity versus φ is obvious for each diffraction, which is ascribed to the noncoplanarity of beam vector and surface normal.[43] It has been reported that in single-crystalline and highly-oriented thin films, the diffraction intensity of the planes parallel to the surface is highly sensitive to the GaN sample orientation.[43] Thus, the comparison of the diffraction peak intensity for the samples grown at different temperatures was not performed. Both the XRD 2θ and φ scan results demonstrate that single-crystalline hexagonal GaN epilayers were deposited on the sapphire at temperatures ranging from 930 to 990 ºC.

X-ray rocking curve (XRC) is a valid method to evaluate the crystallinity of GaN epilayers. The full-width at half-maximum (FWHM) of XRC for the GaN (0002) diffraction peak is used to determine the screw treading dislocations density (TDD) of GaN films, while the FWHM of XRC for the GaN (10-12) peak is sensitive to both the edge and screw TDDs.[44] Figure 3c compares the GaN (0002) XRCs for the GaN epilayers grown at different temperatures. The FWHM values of the GaN (0002) and (10-12) planes were summarized in Table I. For the sample grown at 930 ºC, the FWHMs of XRC for the GaN (0002) and (10-12) diffraction peaks were measured to be 396 and 471 arcsec, respectively, while these two values monotonously decreased to 324 and 443 arcsec for the GaN grown at 960 °C and further decreased to 313 and 390 arcsec for the sample grown at 990 °C, indicating a higher purity and crystallinity for the GaN epilayers grown at higher temperatures. Note that the low FWHM values obtained at 990 °C are similar to those of GaN epilayers grown using the conventional MOCVD and MBE technique.[45] The density of dislocations existing in the GaN layers grown at various growth temperatures was calculated using the following equations:[44, 46]

$$D_{screw} = \frac{\beta_{(0002)}{}^2}{9\, b_{screw}{}^2},\ D_{edge} = \frac{\beta_{(10-12)}{}^2}{9\, b_{edge}{}^2},\ D_{Total} = D_{screw} + D_{edge}, \quad (1)$$

where D_{screw} and D_{edge} are the screw dislocation density and edge dislocation density, $\beta_{(0002)}$ and $\beta_{(10\text{-}12)}$ are the FWHM values of XRC for the GaN (0002) and (10-12) peaks, and b_{screw} (0.5185 nm) and b_{edge} (0.3189 nm) are the Burgers vector lengths of GaN. Figure 3d shows the dislocation density of the as-grown GaN epilayers as a function of deposition temperature. The estimated total dislocation densities D_{Total} for the samples grown at 930, 960, and 990 °C are 8.1×10^8, 6.6×10^8,

and 5.9×10^{8} cm^{-2}, respectively. These findings further indicate that the LMOCVD GaN layers grown at higher temperatures have relatively lower crystalline defects.

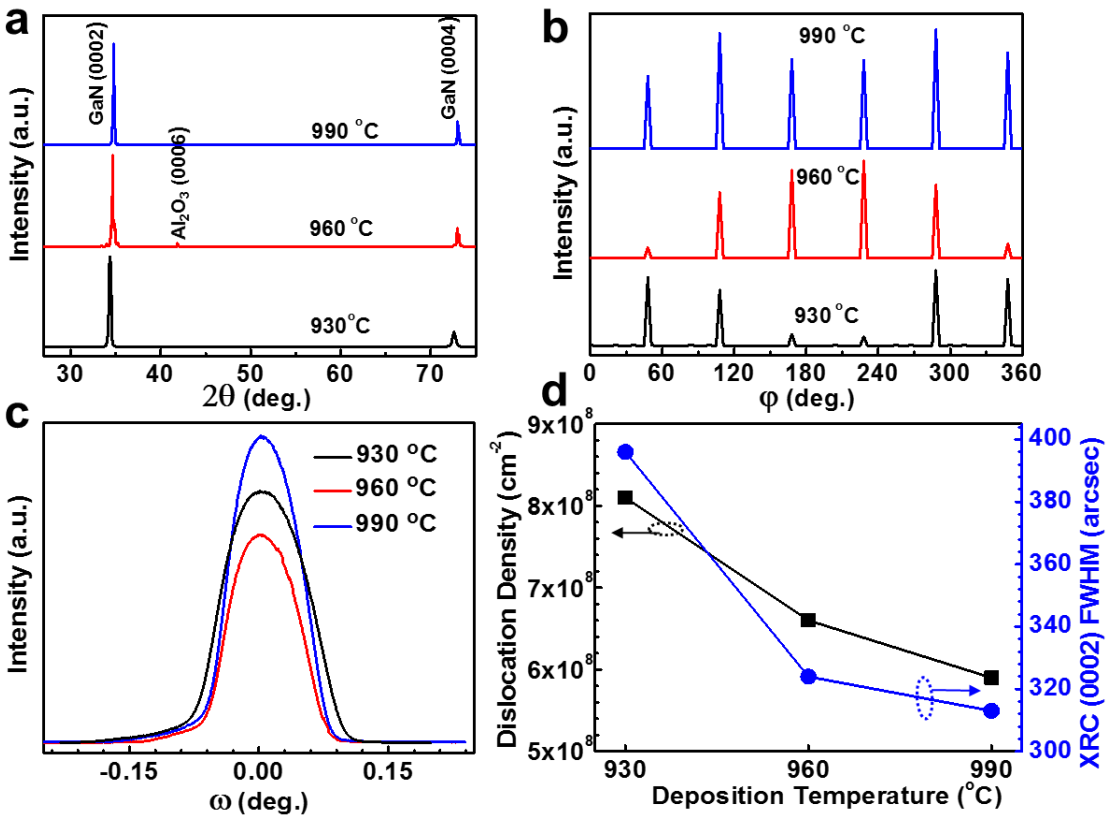

Figure 3. Crystallographic characterization of GaN epilayers grown on sapphire with respect to growth temperatures ranging from 930 to 990 °C. (a) X-ray 2θ scan. (b) X-ray φ scan. (c) XRC curves of the GaN (0002) peak. (d) Temperature dependence of the dislocation density (■) and XRC (0002) FWHM (●) for the GaN epilayers grown on sapphire.

Raman spectroscopy is a popular method to evaluate the quality and residual stress of nitride films.[47] Figure 4a shows the Raman spectra of GaN epilayers grown at different temperatures. Two prominent phonon modes, E_2 (high) and A_1 (LO), are observed in each Raman spectrum. E_2 (high) phonon mode is extremely sensitive to the in-plane stress, from which the residual stress in GaN epilayers can be estimated using the following equation:[48]

$$\sigma = \frac{\Delta\omega}{4.3\ (cm^{-1}\ Gpa^{-1})}, \quad (2)$$

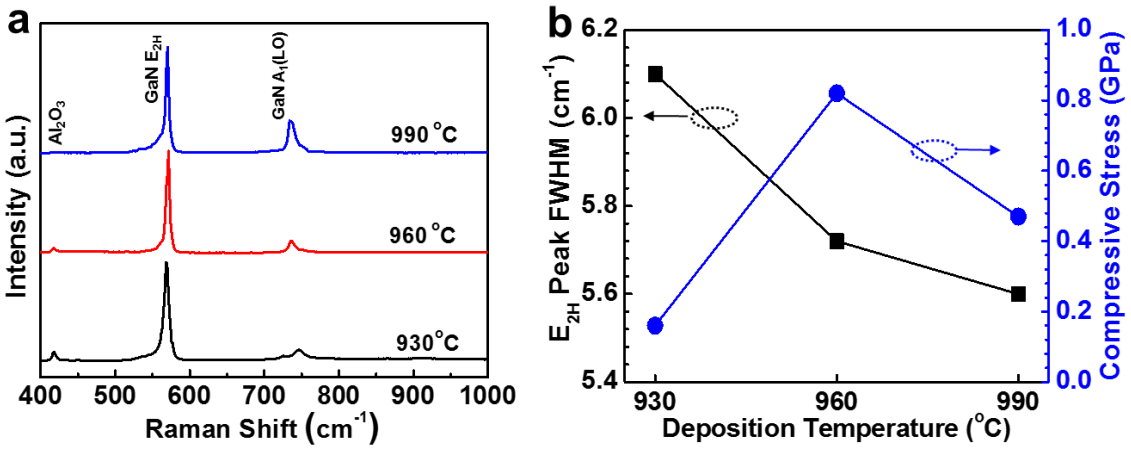

Figure 4. Residual stress evaluation of the GaN epilayers grown on sapphire. (a) Typical Raman spectra of GaN epilayers grown on sapphire at different temperatures. (b) Temperature dependence of FWHM of GaN E_2 (high) peak (■) and film stresses (●).

where σ and $\Delta\omega$ are the biaxial stress and the shift of E_2 (high) peak, respectively. It has been reported that the E_2 (high) peak for the stress-free GaN is located at around 567.6 cm^{-1}.[49] The E_2 (high) phonon peaks of the GaN films grown at 930, 960, and 990 °C are located at 568.7, 571.5, and 570 cm^{-1}, respectively. The E_2 (high) mode peak for all the samples blue-shifts compared to that of the stress-free GaN, which suggests that all GaN films suffer from compressive stress, as predicted for the GaN grown on sapphire substrates.[48] It is known that most of the film stresses arise during sample cooling-down after growth. Figure 4b compares the measured compressive stresses in the GaN epilayers grown at different temperatures. The GaN sample grown at 930 °C shows less in-plane compressive stress compared with the samples grown at higher temperatures of 960 and 990 °C. Additionally, the FWHM value of the E_2 (high) peak for the GaN epilayers

decreased with the increase in the growth temperature, further indicating high crystallinity of the GaN epilayers grown at higher temperatures.

Table I. Summary of characteristics of the LMOCVD GaN epilayers grown on sapphire at different temperatures

No.	Temp. (°C)	RMS (nm)	Bandgap (eV)	E_{2H} (cm^{-1})	σ (Gpa)	(0002)FWHM (arcsec)	(10-12)FWHM (arcsec)	Dislocation density (cm^{-2})	Mobility (cm^2/vs)	Carrier concentration (cm^{-3})
I	930	1.103	3.36	568.7	0.26	396	471	8.1E8	226	8.4×10^{16}
II	960	1.253	3.39	571.5	0.82	324	443	6.6E8	293	5.3×10^{16}
III	990	1.892	3.38	570	0.47	313	390	5.9E8	369	3.1×10^{16}

Electrical and optoelectronic properties of the GaN epilayers were also investigated (Figure 5). Room-temperature Hall effect measurements were performed to study the electrical property of the GaN epilayers, as shown in Figure 5a and Table I. We found that as the growth temperature increases from 930 to 960 and 990 ºC, the mobility increases from 226 to 293 and 369 $cm^2 V^{-1} s^{-1}$ and the carrier concentration decreases from 8.4×10^{16} to 5.3×10^{16} and 3.1×10^{16} cm^{-3}, respectively. The mobility measured in our study is comparable to those reported in several studies for high-quality GaN films deposited using MOCVD and MBE at high temperatures.[50-54] The observed mobility increase with the increased temperature was also reported in the MOCVD GaN films.[53] This can be attributed to the increased film thickness and the improved crystallinity, namely, the crystal defects in the GaN films affect their mobility by scattering the charge carriers.[43, 50-54]

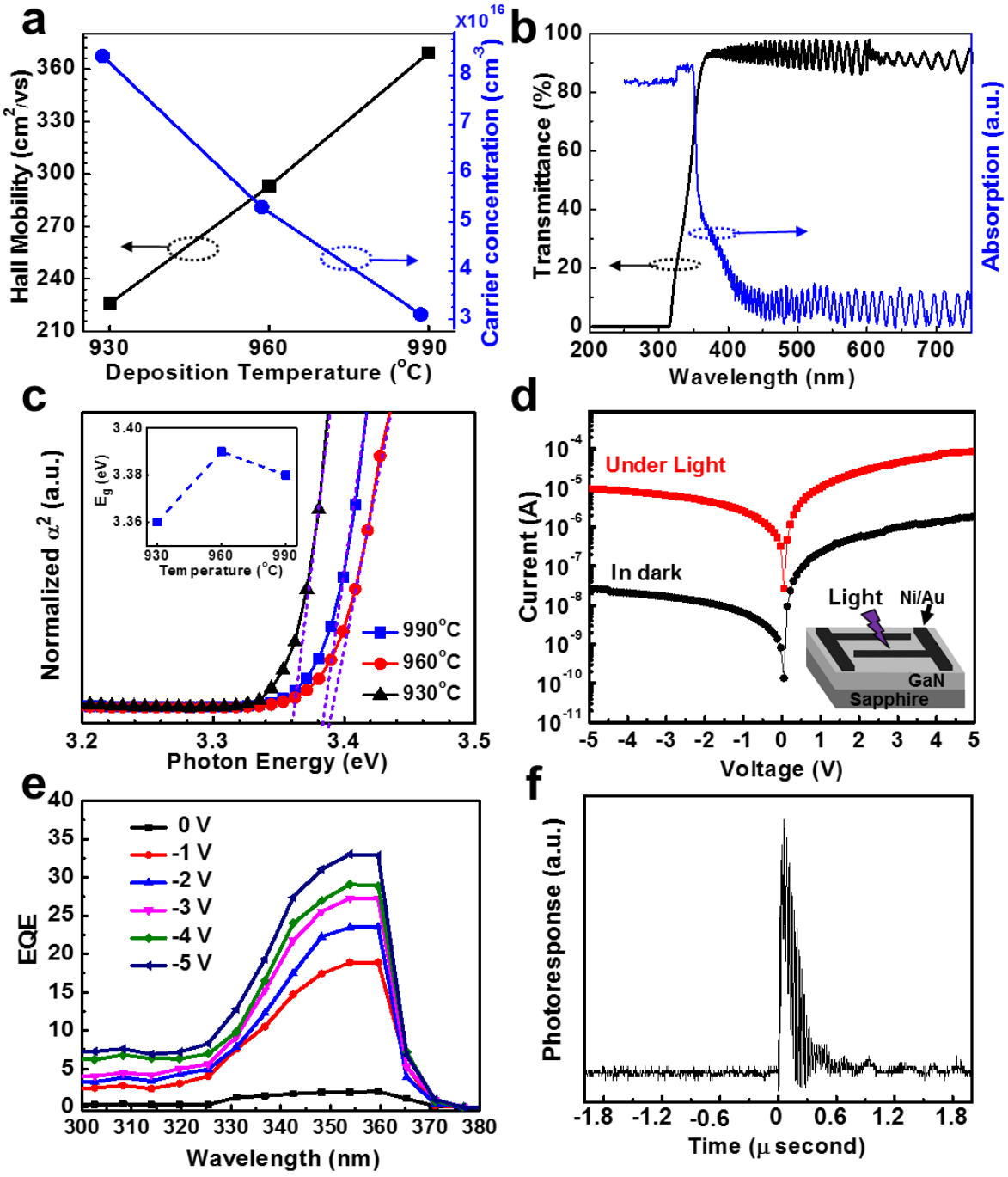

Figure 5. Electrical and optical properties of the LMOCVD GaN epilayers grown on sapphire. (a) Temperature dependence of Hall mobility (black) and resistivity (blue) of the GaN layers. (b) Transmission and absorption spectra of the GaN layers grown at 990 °C. (c) The optical band gap extracted from (b). (d) *I-V* curves of a GaN MSM photodetector under light with power density of 0.1 mW cm^{-2} (red) and in dark (black). The inset in (d) shows the schematic of the device. (e) EQE spectra of the GaN device under reverse bias from -5 to 0 V. (f) Typical transient photocurrent curve of the GaN device under reverse bias of -5 V.

The optical transmission and absorption spectra for the GaN epliayers grown at 990 °C are shown in Figure 5b. The absorption coefficient has been determined from optical transmission data (Figure 5c). The band gap, E_g, of semiconductors with direct band gaps can be estimated using the following equation:[43, 55]

$$\alpha^2 \sim (h\upsilon - E_g), \quad (3)$$

where α is the absorption coefficient, h is the Plank's constant, υ is the frequency, and E_g is the semiconductor band gap.[56] The value of optical band gap can be approximated from a linear extrapolation of square absorption, α^2, to the point of interception with the photon energy axis (Figure 5c). As shown in the inset of Figure 5c, the extracted band gaps, E_g, for GaN epilayers grown at 930, 960 and 990 °C are 3.36, 3.39 and 3.38 eV, respectively. These values are slightly smaller than that of bulk GaN.

The optical quality was further evaluated by fabricating UV photodetector using the as-grown GaN epilayers at 990 °C. GaN UV photodetectors have obtained increasing interest with various applications, such as flame monitoring, biomedicine, and UV astronomy.[57-60] The performance of GaN photodetectors, including responsivity and dark current, is highly dependent on the crystal quality.[61-62] With a high response speed and low dark current characteristics, GaN MSM photodetector has attracted more attentions for UV photodetection applications as compared to GaN photodetectors with other device structures. Additionally, with no n- and p-type doped layers, GaN MSM device has simple fabrication processes (inset in Figure 5d). Figure 5d compares the current-voltage characteristics of the GaN MSM photodetector in dark and under light (light

intensity ~ 0.1 mW cm^{-2}). The dark current of photodetector was ~ 2.7 × 10^{-8} A at a bias voltage of -5 V and increased to ~ 9.4 × 10^{-6} A under light irradiation, revealing an on/off ratio of ~ 348. It is worth to note that the dark current at reverse biases is very low, comparable to that of previously reported GaN UV detectors with the same device structures.[61-62] Figure 5e shows the EQE of UV detector measured at different reverse biases. The device shows a high sensitivity and high responsivity in the UV range that is near the band edge of GaN. However, EQE is quickly reduced with either decreasing or increasing wavelength, which is attributed to the increased electron-hole recombination and the reduced photo-penetration depth.[36-38, 62] The EQE is lower than 2 % at bias of zero, while it increases rapidly as the reverse bias increases and reaches to ~ 36 % at -5 V. The sharp increase of EQE versus reverse bias voltage corresponds to the rapid increase in photocurrent. The responsivity (R) of the device can be measured according to the following equation:[37]

$$R = \frac{EQE}{hc/\lambda}, \quad (4)$$

where h is the Planck's constant, c is the speed of light, and λ is the wavelength of light. The responsivity peak values of ~ 0.0059, 0.069, 0.081, 0.084, and 0.108 AW^{-1} were obtained at biases of 0, 1, 2, 3, 4, and 5 V, respectively. The responsivity value of 0.108 AW^{-1} is comparable to that of commercial GaN UV photodetectors with values in the range of 0.1 to 0.2 AW^{-1}.[38, 63]

Figure 5f shows the response curve of the GaN UV photodetector measured at a reverse bias voltage of -5 V using a pulsed laser with a wavelength of 337 nm as light source, from which the

response time was extracted to be ~ 125 ns. It has been reported that the response time of the device should be limited by the resistor-capacitor time constant but not the GaN crystallinity or carrier mobility.[36] Therefore, the theoretical charge transit time of the UV photodetector was evaluated using the equation below:[36]

$$t_e = \frac{L^2}{\mu_e V}, \quad (5)$$

where μ_e, t_e, L, and V represent carrier mobility, charge transit time, electrode gap spacing, and applied bias, respectively. Using an electron mobility of 369 $cm^2V^{-1}s^{-1}$ for the GaN epilayers grown at 990 °C, L = 10 μm, and the applied voltage -5 V, the charge transit time t_e was calculated to be 0.54 ns, which was much lower than the response time of ~ 125 ns. The 3-dB cut-off frequency (f_{3dB}) was also estimated from the measured response time t_r of 125 ns using [64]

$$f_{3dB} = \frac{0.35}{t_r}. \quad (6)$$

The f_{3db} of the UV GaN photodetector was calculated to be 2.8 MHz. The responsivity of 0.108 AW^{-1}, fast response time of 125 ns, and f_{3db} of 2.8 MHz for the GaN UV photodetector are comparable to those previously reported in literatures,[61-62] suggesting the excellent optical properties of LMOCVD GaN layers grown with high growth rates.

Although the high-performance UV detectors have been realized based on CO_2 laser LMOCVD of the GaN epilayers, there are still some issues to address for the commercialization of GaN epilayer growth via LMOCVD technique. For instance, when compared with MOCVD and MBE

techniques, the sizes of GaN grown by LMOCVD are relatively small due to the small beam size (20 mm in diameter). By adding a beam expander, the laser beam could be extended to cover the whole wafers as well as maintain the required laser fluence for GaN growth, based on which LMOCVD technique is feasible for wafer-scale GaN growth. However, further optimization and design improvement are still required to achieve GaN epi-structures with a homogeneous thickness and high quality over the whole wafers. Overall, CO_2 laser LMOCVD developed in this work is a simple and low-cost method for fast and high-quality GaN epilayer growth, which might provide an extensive application in electronics and optoelectronics.

CONCLUSIONS

In conclusion, we have demonstrated the fast growth of high-quality GaN epilayers with an extremely high growth rate of ~ 25.8 μm/h *via* the CO_2 laser LMOCVD method. The deposition temperature is found to be critical in different aspects of as-grown GaN epilayers, including morphology, crystal structure, optical and optoelectronic properties. The as-grown LMOCVD GaN films have a smooth surface with RMS roughness of ~ 1.9 nm. For the GaN samples grown at 990 °C with high growth rates, the FWHMs of the rocking curve ω-scan for the GaN (0002) line and (10-12) lines are 313 and 390 arcsec, respectively, suggesting the high purity and high crystalline quality. The biaxial compressive stress exists in the as-grown GaN epilayers, as has been evidenced by Raman analysis. We have also fabricated UV photodetectors based on the as-grown GaN epilayers, which exhibit a high responsivity of 0.108 AW^{-1} and a fast response time of 125 ns, indicating the excellent optical properties of GaN layers. These results demonstrate that

LMOCVD technique can produce high-quality GaN epilayers with fast growth rates, opening a new pathway for fabrication of nitride related materials used for next-generation electronics and optoelectronics.

ASSOCIATED CONTENT

Supporting Information. Additional figures illustrate the AFM images of the LMOCVD GaN epilayers grown at 930 and 960 ºC.

AUTHOR INFORMATION

*** Corresponding Author**

E-mail: ylu2@unl.edu, Fax: 402-472-4732.

Notes

[±] Authors contributed equally.

ACKNOWLEDGMENTS

This work was financially supported by the National Science Foundation (NSF CMMI 1129613 and 1265122). Some work was performed in Central Facilities of the Nebraska Center for Materials and Nanoscience, which was supported by the Nebraska Research Initiative.

REFERENCES

(1) Akasaki, I.; Amano, H. Breakthroughs in Improving Crystal Quality of GaN and Invention of the P–N Junction Blue-Light-Emitting Diode. *Jpn. J. Appl. Phys.* **2006,** *45*, 9001–9010.

(2) Asif Khan, M.; Bhattarai, A.; Kuznia, J.; Olson, D. High Electron Mobility Transistor Based on a GaN‐Al x Ga1− x N Heterojunction. *Appl. Phys. Lett.* **1993,** *63*, 1214-1215.

(3) Ponce, F.; Bour, D. Nitride-Based Semiconductors for Blue and Green Light-Emitting Devices. *Nature* **1997,** *386*, 351-359.

(4) Liu, L.; Edgar, J. H. Substrates for Gallium Nitride Epitaxy. *Mater. Sci. Eng. R-Rep.* **2002,** *37*, 61-127.

(5) Fujito, K.; Kubo, S.; Nagaoka, H.; Mochizuki, T.; Namita, H.; Nagao, S. Bulk GaN Crystals Grown by HVPE. *J. Cryst. Growth* **2009,** *311*, 3011-3014.

(6) Hashimoto, T.; Wu, F.; Speck, J. S.; Nakamura, S. A GaN Bulk Crystal with Improved Structural Quality Grown by the Ammonothermal Method. *Nat. Mater.* **2007,** *6*, 568-571.

(7) Yamane, H.; Shimada, M.; Clarke, S. J.; DiSalvo, F. J. Preparation of GaN Single Crystals Using a Na Flux. *Chem. Mater.* **1997,** *9*, 413-416.

(8) Tarsa, E.; Heying, B.; Wu, X.; Fini, P.; DenBaars, S.; Speck, J. Homoepitaxial Growth of GaN under Ga-Stable and N-Stable Conditions by Plasma-Assisted Molecular Beam Epitaxy. *J. Appl. Phys.* **1997,** *82*, 5472-5479.

(9) Heying, B.; Averbeck, R.; Chen, L.; Haus, E.; Riechert, H.; Speck, J. Control of GaN Surface Morphologies using Plasma-Assisted Molecular Beam Epitaxy. *J. Appl. Phys.* **2000,** *88*, 1855-1860.

(10) Boyd, A. R.; Degroote, S.; Leys, M.; Schulte, F.; Rockenfeller, O.; Luenenbuerger, M.; Germain, M.; Kaeppeler, J.; Heuken, M. Growth of GaN/AlGaN on 200 mm Diameter Silicon (111) Wafers by MOCVD. *Phys. Status Solidi C* **2009,** *6*, 1045–1048.

(11) Nakamura, S.; Harada, Y.; Seno, M. Novel Metalorganic Chemical Vapor Deposition System for GaN Growth. *Appl. Phys. Lett.* **1991,** *58*, 2021-2023.

(12) Heikman, S.; Keller, S.; DenBaars, S. P.; Mishra, U. K. Growth of Fe Doped Semi-Insulating GaN by Metalorganic Chemical Vapor Deposition. *Appl. Phys. Lett.* **2002,** *81*, 439-441.

(13) Iga, R.; Sugiura, H.; Yamada, T. Selective Growth of III-V Semiconductor Compounds by Laser-Assisted Epitaxy. *Semicond. Sci. Technol.* **1993,** *8*, 1101-1111.

(14) Shinn, G. B.; Gillespie, P.; Wilson Jr, W.; Duncan, W. M. Laser-Assisted Metalorganic Chemical Vapor Deposition of Zinc Selenide Epitaxial Films. *Appl. Phys. Lett.* **1989,** *54*, 2440-2442.

(15) Allen, S. Laser Chemical Vapor Deposition: A Technique for Selective Area Deposition. *J. Appl. Phys.* **1981,** *52*, 6501-6505.

(16) Herman, I. P. Laser-Assisted Deposition of Thin Films from Gas-Phase and Surface-Adsorbed Molecules. *Chem. Rev.* **1989,** *89*, 1323-1357.

(17) Duty, C.; Jean, D.; Lackey, W. Laser Chemical Vapour Deposition: Materials, Modelling, and Process Control. *Int. Mater. Rev.* **2001,** *46*, 271-287.

(18) Keramatnejad, K.; Zhou, Y. S.; Gao, Y.; Rabiee Golgir, H.; Wang, M.; Jiang, L.; Silvain, J.-F.; Lu, Y. F. Skin Effect Mitigation in Laser Processed Multi-Walled Carbon Nanotube/Copper Conductors. *J. Appl. Phys.* **2015,** *118*, 154311.

(19) Keramatnejad, K.; Zhou, Y.; Li, D.; Rabiee Golgir, H.; Huang, X.; Zhou, Q.; Song, J.; Ducharme, S.; Lu, Y.

Laser-Assisted Nanowelding of Graphene to Metals: An Optical Approach Toward Ultralow Contact Resistance. *Adv. Mater. Interfaces* **2017**.

(20) Keramatnejad, K.; Rabiee Golgir, H.; Zhou, Y.; Li, D.; Huang, X.; Lu, Y. *Reducing Graphene-Metal Contact Resistance via Laser Nano-welding*, Proc. of SPIE **2017**.

(21) Zhou, B.; Li, Z.; Tansley, T.; Butcher, K. Growth Mechanisms in Excimer Laser Photolytic Deposition of Gallium Nitride at 500° C. *J. Cryst. Growth* **1996,** *160*, 201-206.

(22) Iwanaga, T.; Hanabusa, M. CO_2 Laser CVD of Disilane. *Jpn. J. Appl. Phys.* **1984,** *23*, 473-475.

(23) Thirugnanam, P.; Xiong, W.; Mahjouri-Samani, M.; Fan, L. S.; Raju, R.; Mitchell, M.; Gao, Y.; Krishnan, B.; Zhou, Y. S.; Jiang, L. Lu, Y. F. Rapid Growth of M-Plane Oriented Gallium Nitride Nanoplates on Silicon Substrate Using Laser-Assisted Metal Organic Chemical Vapor Deposition. *Cryst. Growth Des.* **2013,** *13*, 3171-3176.

(24) Besling, W.; Goossens, A.; Meester, B.; Schoonman, J. Laser-Induced Chemical Vapor Deposition of Nanostructured Silicon Carbonitride Thin Films. *J. Appl. Phys.* **1998,** *83*, 544-553.

(25) Rabiee Golgir, H.; Gao, Y.; Zhou, Y. S.; Fan, L.; Thirugnanam, P.; Keramatnejad, K.; Jiang, L.; Silvain, J.-F. o.; Lu, Y. F. Low-Temperature Growth of Crystalline Gallium Nitride Films Using Vibrational Excitation of Ammonia Molecules in Laser-Assisted Metalorganic Chemical Vapor Deposition. *Cryst. Growth Des.* **2014,** *14*, 6248-6253.

(26) Golgir, H. R.; Zhou, Y. S.; Li, D. W.; Keramatnejad, K.; Xiong, W.; Wang, M. M.; Jiang, L. J.; Huang, X.; Jiang, L.; Silvain, J. F.; Lu, Y. F. Resonant and Nonresonant Vibrational Excitation of Ammonia Molecules in the Growth of Gallium Nitride Using Laser-Assisted Metal Organic Chemical Vapour Deposition. *J. Appl. Phys.* **2016,** *120*, 105303.

(27) Lu, Y.; Golgir, H. R.; Zhou, Y. Growth of Nitride Films. US Patent 20,160,340,783, **2016**.

(28) Meunier, M.; Flint, J.; Haggerty, J.; Adler, D. Laser-Induced Chemical Vapor Deposition of Hydrogenated Amorphous Silicon. I. Gas-Phase Process Model. *J. Appl. Phys.* **1987,** *62*, 2812-2821.

(29) Golgir, H. R.; Gao, Y.; Zhou, Y.; Fan, L.; Keramatnejad, K.; Lu, Y. *Effect of Laser-Assisted Resonant Excitation on the Growth of GaN Films*, Proceedings of the 33nd International Congress on Applications of Lasers and Electro-Optics (ICALEO), **2014**.

(30) Thirugnanam, P.; Zhou, Y.; Golgir, H.; Gao, Y.; Lu, Y. *Synthesis of Gallium Nitride Nanoplates Using Laser-Assisted Metal Organic Chemical Vapor Deposition*, Proceedings of the 32nd International Congress on Applications of Lasers and Electro-Optics (ICALEO), **2013**.

(31) Park, M.; Maria, J.-P.; Cuomo, J.; Chang, Y.; Muth, J.; Kolbas, R.; Nemanich, R.; Carlson, E.; Bumgarner, J. X-Ray and Raman Analyses of GaN Produced by Ultrahigh-Rate Magnetron Sputter Epitaxy. *Appl. Phys. Lett.* **2002,** *81*, 1797-1799.

(32) Schiaber, Z. S.; Leite, D. M.; Bortoleto, J. R.; Lisboa-Filho, P. N.; da Silva, J. H. Effects of Substrate Temperature, Substrate Orientation, and Energetic Atomic Collisions on the Structure of GaN Films Grown by Reactive Sputtering. *J. Appl. Phys.* **2013,** *114*, 183515.

(33) Hao, M.; Ishikawa, H.; Egawa, T. Formation Chemistry of High-Density Nanocraters on the Surface of Sapphire Substrates with an In-Situ Etching and Growth Mechanism of Device-Quality GaN Films on the Etched Substrates. *Appl. Phys. Lett.* **2004,** *84*, 4041-4043.

(34) Yadav, B. S.; Major, S.; Srinivasa, R. Growth and Structure of Sputtered Gallium Nitride Films. *J. Appl. Phys.* **2007,** *102*, 073516.

(35) Lahreche, H.; Leroux, M.; Laügt, M.; Vaille, M.; Beaumont, B.; Gibart, P. Buffer Free Direct Growth of GaN on 6H–SiC by Metalorganic Vapor Phase Epitaxy. *J. Appl. Phys.* **2000,** *87*, 577-583.
(36) Fang, Y.; Huang, J. Resolving Weak Light of Sub‐Picowatt per Square Centimeter by Hybrid Perovskite Photodetectors Enabled by Noise Reduction. *Adv. Mater.* **2015,** *27*, 2804-2810.
(37) Guo, F.; Xiao, Z.; Huang, J. Fullerene Photodetectors with a Linear Dynamic Range of 90 dB Enabled by a Cross-Linkable Buffer Layer. *Adv. Opt. Mater.* **2013,** *1*, 289-294.
(38) Guo, F.; Yang, B.; Yuan, Y.; Xiao, Z.; Dong, Q.; Bi, Y.; Huang, J. A Nanocomposite Ultraviolet Photodetector Based on Interfacial Trap-Controlled Charge Injection. *Nat. Nanotechnol.* **2012,** *7*, 798-802.
(39) Li, J.; Chen, Z.; Jiao, Q.; Feng, Y.; Jiang, S.; Chen, Y.; Yu, T.; Li, S.; Zhang, G. Silane Controlled Three Dimensional GaN Growth and Recovery Stages on a Cone-Shape Nanoscale Patterned Sapphire Substrate by MOCVD. *Cryst. Eng. Comm.* **2015,** *17*, 4469-4474.
(40) Gunning, B. P.; Clinton, E. A.; Merola, J. J.; Doolittle, W. A.; Bresnahan, R. C. Control of Ion Content and Nitrogen Species Using a Mixed Chemistry Plasma for GaN Grown at Extremely High Growth Rates > 9 μm/h by Plasma-Assisted Molecular Beam Epitaxy. *J. Appl. Phys.* **2015,** *118*, 155302.
(41) Gibart, P. Metal Organic Vapour Phase Epitaxy of GaN and Lateral Overgrowth. *Rep. Prog. Phys.* **2004,** *67*, 667–715.
(42) Kim, J.; Bayram, C.; Park, H.; Cheng, C.-W.; Dimitrakopoulos, C.; Ott, J. A.; Reuter, K. B.; Bedell, S. W.; Sadana, D. K. Principle of Direct Van Der Waals Epitaxy of Single-Crystalline Films on Epitaxial Graphene. *Nat. Commun.* **2014,** *5*, 4836.
(43) Motamedi, P.; Cadien, K. Structure-Property Relationship and Interfacial Phenomena in GaN Grown on C-Plane Sapphire via Plasma-Enhanced Atomic Layer Deposition. *RSC Adv.* **2015,** *5*, 57865-57874.
(44) Moram, M.; Vickers, M. X-Ray Diffraction of III-Nitrides. *Rep. Prog. Phys.* **2009,** *72*, 036502.
(45) Collazo, R.; Mita, S.; Aleksov, A.; Schlesser, R.; Sitar, Z. Growth of Ga-and N-Polar Gallium Nitride Layers by Metalorganic Vapor Phase Epitaxy on Sapphire Wafers. *J. Cryst. Growth* **2006,** *287*, 586-590.
(46) Kushvaha, S.; Kumar, M. S.; Shukla, A.; Yadav, B.; Singh, D. K.; Jewariya, M.; Ragam, S.; Maurya, K. Structural, Optical and Electronic Properties of Homoepitaxial GaN Nanowalls Grown on GaN Template by Laser Molecular Beam Epitaxy. *RSC Adv.* **2015,** *5*, 87818-87830.
(47) Kuball, M. Raman Spectroscopy of GaN, AlGaN and AlN for Process and Growth Monitoring/Control. *Surf. Interface Anal.* **2001,** *31*, 987-999.
(48) Tripathy, S.; Chua, S.; Chen, P.; Miao, Z. Micro-Raman Investigation of Strain in GaN and Al x Ga 1− x N/GaN Heterostructures Grown on Si (111). *J. Appl. Phys.* **2002,** *92*, 3503-3510.
(49) Goni, A.; Siegle, H.; Syassen, K.; Thomsen, C.; Wagner, J.-M. Effect of Pressure on Optical Phonon Modes and Transverse Effective Charges in GaN and AlN. *Phys. Rev. B* **2001,** *64*, 035205.
(50) Ko, C.-H.; Chang, S.-J.; Su, Y.-K.; Lan, W.-H.; Chen, J. F.; Kuan, T.-M.; Huang, Y.-C.; Chiang, C.-I.; Webb, J.; Lin, W.-J. On the Carrier Concentration and Hall Mobility in GaN Epilayers. *Jpn. J. Appl. Phys.* **2002,** *41*, 226-228.
(51) Meister, D.; Böhm, M.; Topf, M.; Kriegseis, W.; Burkhardt, W.; Dirnstorfer, I.; Rösel, S.; Farangis, B.; Meyer, B.; Hoffmann, A. A Comparison of the Hall-Effect and Secondary Ion Mass Spectroscopy on the Shallow Oxygen Donor in Unintentionally Doped GaN Films. *J. Appl. Phys.* **2000,** *88*, 1811-1817.
(52) Hwang, C.; Schurman, M.; Mayo, W.; Lu, Y.; Stall, R.; Salagaj, T. Effect of Structural Defects and Chemical Impurities on Hall Mobilities in Low Pressure MOCVD Grown GaN. *J. Electron. Mater.* **1997,** *26*, 243-251.

(53) Wang, T.; Shirahama, T.; Sun, H.; Wang, H.; Bai, J.; Sakai, S.; Misawa, H. Influence of Buffer Layer and Growth Temperature on the Properties of an Undoped GaN Layer Grown on Sapphire Substrate by Metalorganic Chemical Vapor Deposition. *Appl. Phys. Lett.* **2000,** *76*, 2220-2222.
(54) Kordoš, P.; Javorka, P.; Morvic, M.; Betko, J.; Van Hove, J.; Wowchak, A.; Chow, P. Conductivity and Hall-Effect in Highly Resistive GaN Layers. *Appl. Phys. Lett.* **2000,** *76*, 3762-3764.
(55) Xiao, R.; Liao, H.; Cue, N.; Sun, X.; Kwok, H. S. Growth of C-Axis Oriented Gallium Nitride Thin Films on an Amorphous Substrate by the Liquid-Target Pulsed Laser Deposition Technique. *J. Appl. Phys.* **1996,** *80*, 4226-4228.
(56) Klingshirn, C. F. *Semiconductor Optics*; Springer Science & Business Media: Berlin, **2012**.
(57) Razeghi, M.; Rogalski, A. Semiconductor Ultraviolet Detectors. *J. Appl. Phys.* **1996,** *79*, 7433-7473.
(58) Ozbay, E.; Biyikli, N.; Kimukin, I.; Kartaloglu, T.; Tut, T.; Aytur, O. High-Performance Solar-Blind Photodetectors Based on Al/sub x/Ga/sub 1-x/N Heterostructures. *IEEE J. Sel. Topics Quantum Electron.* **2004,** *10*, 742-751.
(59) Kamran, K.; Saeid, K.; Farshid, R.; Fatemeh, K. *Highly Sensitive Porous PtSi/Si UV Detector with High Selectivity*, Micro and Nanoelectronics (RSM), 2013 IEEE Regional Symposium on, IEEE: **2013**; pp 194-196.
(60) Keramatnejad, K.; Khorramshahi, F.; Khatami, S.; Asl-Soleimani, E. Optimizing UV Detection Properties of N-ZnO Nanowire/P-Si Heterojunction Photodetectors by Using a Porous Substrate. *Opt. Quant. Electron.* **2015,** *47*, 1739-1749.
(61) Sun, X.; Li, D.; Jiang, H.; Li, Z.; Song, H.; Chen, Y.; Miao, G. Improved Performance of GaN Metal-Semiconductor-Metal Ultraviolet Detectors by Depositing SiO_2 Nanoparticles on a GaN Surface. *Appl. Phys. Lett.* **2011,** *98*, 121117.
(62) Li, D.; Sun, X.; Song, H.; Li, Z.; Chen, Y.; Miao, G.; Jiang, H. Influence of Threading Dislocations on GaN-Based Metal-Semiconductor-Metal Ultraviolet Photodetectors. *Appl. Phys. Lett.* **2011,** *98*, 011108.
(63) Monroy, E.; Omnès, F.; Calle, F. Wide-Bandgap Semiconductor Ultraviolet Photodetectors. *Semicond. Sci. Technol.* **2003,** *18*, R33-R51.
(64) Marks, R.; Halls, J.; Bradley, D.; Friend, R.; Holmes, A. The Photovoltaic Response in Poly (P-Phenylene Vinylene) Thin-Film Devices. *J. Phys. Condens. Matter* **1994,** *6*, 1379-1394.

(For Table of Contents Use Only)

Fast Growth of GaN Epilayers via Laser-Assisted Metal Organic Chemical Vapor Deposition for Ultraviolet Photodetector Applications

*Hossein Rabiee Golgir, Da Wei Li, Kamran Keramatnejad, Qi Ming Zou, Jun Xiao, Fei Wang, Lan Jiang, Jean-François Silvain, and Yong Feng Lu**

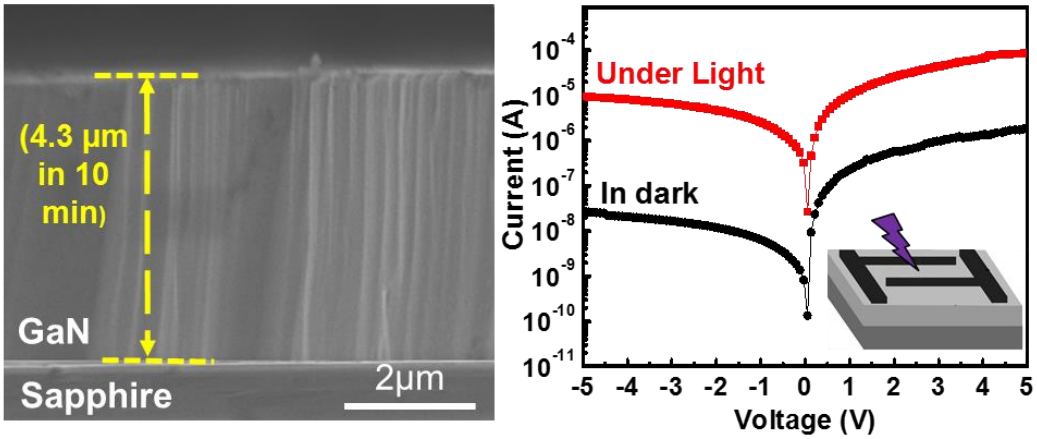

We have demonstrated the fast growth of high-quality GaN epilayers on sapphire (0001) substrate with an extremely high growth rate of ~ 25.8 μm/h *via* a CO_2 laser-assisted metal organic chemical vapor deposition, which provides a simple and cost-effective means toward high-performance GaN-based ultraviolet photodetectors.